Deep Convolutional Neural Network-Based Lymph Node Metastasis Prediction for Colon Cancer Using Histopathological Images

Min Seob Kwak[1]*, Hun Hee Lee[1], Jae Min Yang[2], Jae Myung Cha[1], Jung Won Jeon[1], Jin Young Yoon[1] and Ha Il Kim[1]

[1] Department of Internal Medicine, Kyung Hee University Hospital at Gangdong, Kyung Hee University College of Medicine, Seoul, South Korea, [2] Department of Computer Science and Engineering, Konkuk University, Seoul, South Korea

Background: Human evaluation of pathological slides cannot accurately predict lymph node metastasis (LNM), although accurate prediction is essential to determine treatment and follow-up strategies for colon cancer. We aimed to develop accurate histopathological features for LNM in colon cancer.

Methods: We developed a deep convolutional neural network model to distinguish the cancer tissue component of colon cancer using data from the tissue bank of the National Center for Tumor Diseases and the pathology archive at the University Medical Center Mannheim, Germany. This model was applied to whole-slide pathological images of colon cancer patients from The Cancer Genome Atlas (TCGA). The predictive value of the peri-tumoral stroma (PTS) score for LNM was assessed.

Results: A total of 164 patients with stages I, II, and III colon cancer from TCGA were analyzed. The mean PTS score was 0.380 ($\pm$ SD = 0.285), and significantly higher PTS scores were observed in patients in the LNM-positive group than those in the LNM-negative group ($P < 0.001$). In the univariate analyses, the PTS scores for the LNM-positive group were significantly higher than those for the LNM-negative group ($P < 0.001$). Further, the PTS scores in lymphatic invasion and any one of perineural, lymphatic, or venous invasion were significantly increased in the LNM-positive group ($P < 0.001$ and $P < 0.001$).

Conclusion: We established the PTS score, a simplified reproducible parameter, for predicting LNM in colon cancer using computer-based analysis that could be used to guide treatment decisions. These findings warrant further confirmation through large-scale prospective clinical trials.

Keywords: prognostic score, deep learning–artificial neural network, colorectal cancer, metastasis, histology

INTRODUCTION

Colon cancer is a major cause of morbidity and mortality worldwide, and its occurrence is expected to increase significantly over the next few years (1, 2). In recent years, the number of dysplastic and colon cancer cases has increased, resulting in increased awareness and the introduction of screening and surveillance programs for colon cancer (3, 4). The presence of lymph node metastasis (LNM) is a crucial prognostic factor to determine whether patients with early-stage colon cancer should undergo additional surgery after local endoscopic treatment and whether adjuvant chemotherapy is necessary after surgical resection for those in the advanced stages (5–7).

Currently, clinicians make important treatment decisions through nodal status evaluation based only on limited radiological examinations, such as ultrasound and computed tomography, and on manual evaluations of a few histological features *via* light microscopy. However, qualitative evaluation of pathological features exclusively (such as histologic type, depth of tumor invasion, and tumor grades) is insufficient for predicting the presence of LNM in patients with colon cancer; inconsistent determinations among experienced pathologists have been noted even with the best-characterized histopathological features. Furthermore, micro-metastasis (8, 9), the presence of minimal cancer cells in regional lymph nodes that pathological examination cannot detect, is observed through immunohistochemistry and molecular genetic evaluation in up to 50% of patients with node-negative colon cancer even after radical surgery, aside from local endoscopic treatment being unable to provide an accurate status of regional lymph nodes (10–12).

Recently, computer-aided image analysis in histopathology evaluations has been shown to offer efficient, accurate, and consistent quantitative feature extraction and also provides decision-making support to ensure diagnostic consistency (13, 14).

Therefore, the purpose of this study is to identify a pathological parameter for reliable and accurate assessment of LNM using a deep convolution neural network (CNN) model that can better stratify patients with colon cancer.

MATERIALS AND METHODS

Histopathology Image Resource for Predictive Parameter

All available digital whole-slide stained high-resolution histopathological images of colorectal cancer (CRC) were obtained from the Genomic Data Commons Data Portal of the National Cancer Institute (https://portal.gdc.cancer.gov/). Pathology slides for the presence and extent of tumors and various tissue components were manually reviewed by a board-certified pathologist (K.Y.W.). The number of pathology image slides publicly available from The Cancer Genome Atlas (TCGA) cohort varied, ranging from one to eight slides (a majority of patients had only one representative slide of the tumor specimen). At model inference and evaluation, only one representative slide for each patient was used in the analysis.

Patients with rectal cancer were excluded because rectal cancer differs from colon cancer in its outcome patterns, such as local relapse or metastasis in the disease course after curative surgery (15). Slides with tissue folds, torn tissues, inadequately stained tissues, or other artifacts as well as slides without any tumor tissue were excluded. Based on the American Joint Committee on Cancer (AJCC) staging system, the patients with colon cancer were divided into LNM-positive (stage III) and LNM-negative (stage I and stage II) groups, according to the pathological presence or absence of LNM (16), respectively. Extramural tumor deposits (EMTDs), including lymphatic invasion (LI), venous invasion (VI), perineural invasion (PI), and any of the aforementioned features (AnyI), were also evaluated (17). This study was reviewed and approved by the Institutional Review Board of the Kyung Hee University Hospital at Gangdong (KHNMC IRB 2020-09-025). The need for informed consent was waived because all data used in this study were de-identified.

Training and Testing of Neural Networks

For the training of our CNN model, we used a training image set comprising 100,000 image patches (224×224 pixels and $0.5\ \mu m$/pixel), with an approximately equal number of images for the following seven tissue classes: normal colon mucosa, stroma, lymphocytes, mucus, adipose tissue, smooth muscle, and colon cancer epithelium; this image set is publicly available at http://dx.doi.org/10.5281/zenodo.1214456. We conducted the image segmentation using the multi-threshold technique (18). Our network architecture for the auto-segmentation of tumor-microenvironment-related features in colon cancer histology is based on the U-Net architecture (19) because this architecture was initially proposed to improve the performance of fine segmentation and localization, particularly for biomedical images. For images with heights and widths less than the target size, we padded all image patches with "reflect padding" to obtain a size of 512×512; the padded voxels were acquired by mirroring the existing images. All images were normalized using the Macenko method (20) and were preprocessed prior to thresholding *via* histogram normalization, in order to standardize the intensities of each RGB channel in the range of 0 to 255 (21). The threshold values were empirically selected, and visual validation was conducted by an experienced pathologist. Among the generated image patches, 80% were used to train our model with forward and backward propagation. To build high-performance network architectures, we divided the remaining data into a 10% validation set and 10% testing set. We used Adam to minimize the cross-entropy loss during stochastic optimization and the adaptive momentum algorithm for smooth convergence (22). Training was terminated when the mean Dice similarity coefficient (DSC) for the validation dataset did not increase by at least 0.1% after 10 additional epochs from its epoch with the best performance. The best model was generated in the epoch with the highest mean DSC. Training was implemented with the Keras library on a parallel computing architecture, using an Intel Core i9-7960 CPU (2.8 GHz) and a two-GPU-enabled Nvidia GeForce RTX Titan graphics card (24 GB of memory).

Histological Microenvironmental Feature Extraction

Morphological image processing (MIP) involves a collection of non-linear operations related to the shape or morphology of features in an image (23). The images may contain numerous imperfections. In particular, the binary regions produced by simple thresholding are distorted by noise and texture. To identify the features of interest in whole-slide images after removing inevitable imperfections, feature extraction of the histological microenvironment was performed based on MIP, which is generated by optimizing the structuring element (SE) over the image in an activity similar to convolution (23). At each pixel position, an individual operation was applied between the corresponding SEs and the matrix data of each pathology image. The successive operations of morphological erosion and dilation of MIP were performed based on the nature of the SE (24). The PTS area was calculated as the sum of pixels of stroma tissue within the tumor region boundaries derived from MIP. Then, it was adjusted by the tumor area computed using the total number of annotated pixels originating from cancer. The PTS score is defined as [PTS area]/[tumor area]. An overview schematic of the analysis is displayed in **Supplementary Figure 1**.

Statistical Analysis

All analyses were performed with R statistical software (version 4.0.0) and Python (version 3.6.9). Demographic differences between the two groups were tested using the Student's t-test and Pearson chi-square test. To assess the performance of the proposed parameter, we obtained the area under the curve of the receiver operating characteristic (ROC), a distribution of the performance metric. We used an unadjusted logistic regression method and calculated odds ratios (ORs) and their 95% confidence intervals (CIs) to assess statistical associations between independent variables and outcomes. Two-sided $P \leq 0.05$ was considered to be statistically significant.

RESULTS

Image Processing

A total of 591 patients (600 slides) with CRC in TCGA data were collected, of which about 153 patients (154 slides) were excluded from the study because they were diagnosed with rectal cancer. After excluding 210 patients (217 slides) with inadequate image data, such as poor image quality, bad H&E staining (i.e., too weak or too strong), duplicated images, and artifacts, and 64 patients (65 slides) with distant metastases, 164 patients (164 slides), with a diagnosis of colon cancer in stages I, II, and III based on the seventh edition of the AJCC, were analyzed (25). The image data processing workflow is shown in **Figure 1**.

Patient Characteristics

A total of 98 patients (59.8%) were in the LNM-negative group, while the LNM-positive group accounted for 40.2% (**Table 1**). The patients without LNM {mean age 66.8 years [standard deviation (SD), 13.1]} were older than those with LNM [mean

FIGURE 1 | Workflow of image data processing.
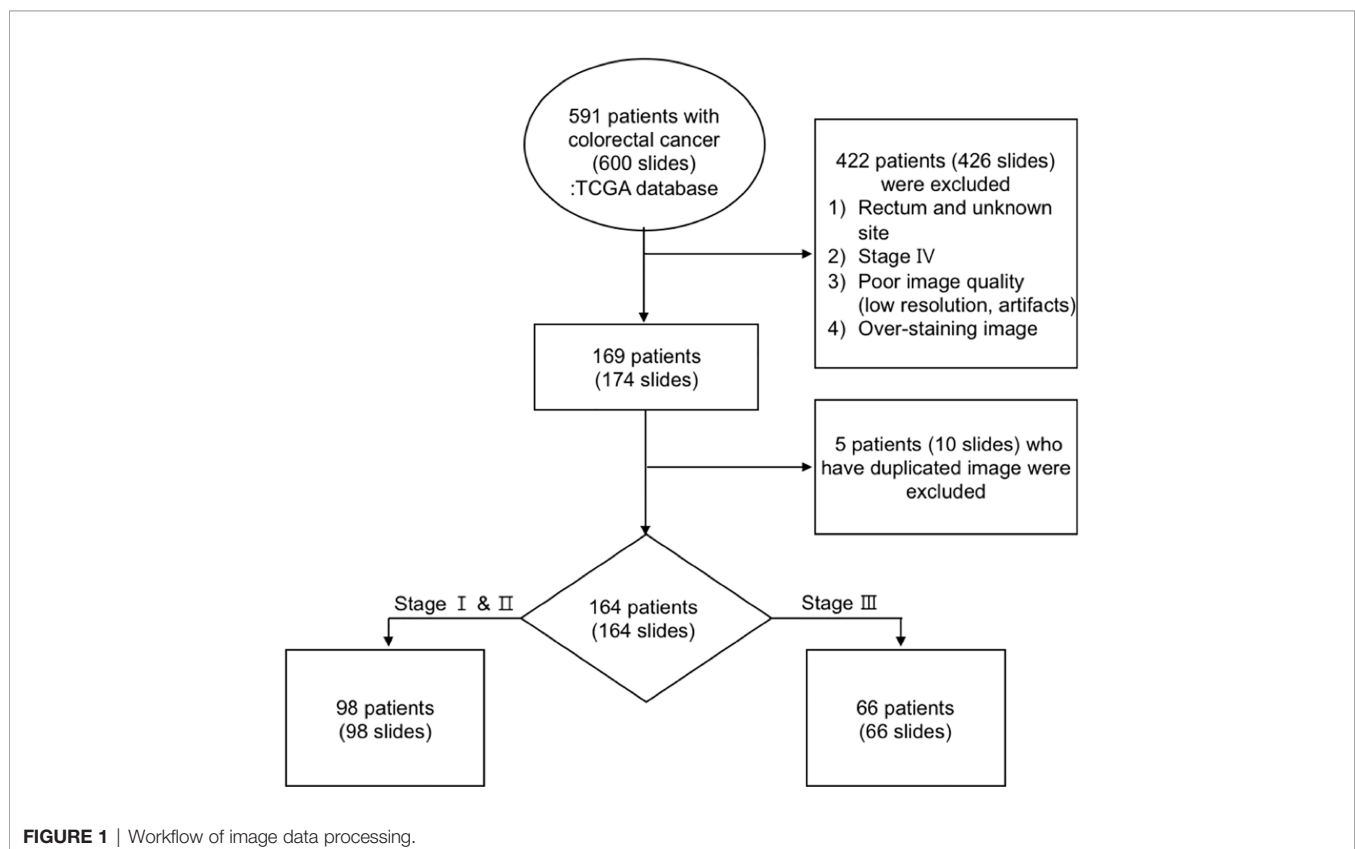
TABLE 1 | Clinical and pathologic characteristics of the included patients with colon cancer.

		LNM-negative (N = 98)	LNM-positive (N = 66)	P-value
Age, yr, mean (SD)		66.8 (13.1)	61.8 (13.6)	0.021
Sex, n (%)				0.777
	M	48 (49.0)	30 (45.5)	
	F	50 (51.0)	36 (54.5)	
Race, n (%)				0.075
	Asian	7 (7.1)	0 (0.0)	
	Black or African American	23 (23.5)	19 (28.8)	
	White	68 (69.4)	47 (71.2)	
T stage, n (%)				<0.001
	T0	1 (1.0)	0 (0.0)	
	T1	4 (4.1)	1 (1.5)	
	T2	25 (25.5)	2 (3.0)	
	T3	63 (64.3)	53 (80.3)	
	T4	5 (5.1)	10 (15.2)	
N stage, n (%)				<0.001
	N0	98 (100.0)	0 (0.0)	
	N1	0 (0.0)	46 (69.7)	
	N2	0 (0.0)	20 (30.3)	
LI, n (%)				<0.001
	Yes	11 (11.2)	42 (63.6)	
	No	79 (80.6)	22 (33.3)	
	NA	8 (8.2)	2 (3.0)	
PI, n (%)				
	Yes	12 (12.2)	13 (19.7)	0.208
	No	58 (59.2)	32 (48.5)	
	NA	28 (28.6)	21 (31.8)	
VI, n (%)				<0.001
	Yes	13 (13.3)	25 (37.9)	
	No	76 (77.6)	37 (56.1)	
	NA	9 (9.2)	4 (6.1)	
AnyI, n (%)				
	Yes	23 (23.5)	45 (68.2)	<0.001
	No	68 (69.4)	20 (30.3)	
	NA	7 (7.1)	1 (1.5)	

SD, standard deviation; NA, not applicable; LI, lymphatic invasion; PI, perineural invasion; VI, venous invasion; AnyI, any feature of extramural tumor deposits.

age 61.8 years (SD, 13.6), $P = 0.021$] (**Table 1**). Among the patients with LNM, 54.5% were female, and 45.5% were male (**Table 1**). A total of 66 patients with LNM had T3 (80.3%) and T4 (15.2%) primary tumors, while T1 and T2 (4.5%) tumors were less frequent ($P < 0.001$). According to the data, LI and VI were more likely to occur in the patients with LNM, and 42 cases (63.6%) and 25 cases (37.9%), respectively, were observed in our sample (all $P < 0.001$, **Table 1**). The details of the patients' clinicopathological summaries are shown in **Table 1**.

Evaluation of Histological Image Segmentation Using CNN

In **Supplementary Figure 2**, we present the curves of training accuracy, loss, and test accuracy over epochs. The training and test accuracy curves converge on approaching 56 epochs, where training met our criterion for termination. The proposed model achieved high segmentation performance, scoring a test mean DSC of 0.892. We observed balanced class performance for all the neural networks we tested (including other architectures),

with DSC values of 0.938, 0.968, 0.841, 0.732, 0.928, 0.815, and 0.930 for adipose tissue, lymphocytes, mucus, smooth muscle, normal colon mucosa, stroma, and colon cancer epithelium, respectively (**Table 2**). A representative image of the corresponding segmented classes from the designed model is shown in **Figure 2**.

PTS Score for Prognostic Factor

Figure 3 shows the PTS and tumor segmented through MIP. The mean score for the PTS was 0.380 (SD 0.285), and significantly higher PTS scores were observed in the LNM-positive group than in the LNM-negative group ($P < 0.001$) (**Table 3**). In the univariate analyses, the PTS scores for patients of the LNM-positive group were significantly higher than the scores of those of the LNM-negative group (OR 26.654; CIs 5.677–196.987, $P < 0.001$) (**Table 3**). The PTS score had a moderate ability to identify the presence of LNM in colon cancer (AUC 0.677; CIs 0.593–0.760) (**Supplementary Figure 3**).

Compared with the patients who did not have EMTDs, the PTS scores in LI and AnyI were significantly higher in the patients with colon cancer ($P < 0.001$ for both), while no significant association was identified between the PTS score and LI, VI, or AnyI (**Table 3** and **Supplementary Figure 4**). Furthermore, we performed subgroup analysis to evaluate the effect of the stage of tumor penetration (T-stage) on the predictive value of the PTS scores. Comparing the PTS scores for patients in the T3–4 stages, the univariate logistic regression model demonstrated that the ORs were 16.415 (CIs 2.912–124.106, $P = 0.003$) for LI, 0.549 (CIs 0.029–6.678, $P = 0.659$) for PI, 3.106 (CIs 0.643–15.753, $P = 0.156$) for VI, and 5.529 (CIs 1.123–34.790, $P = 0.049$) for AnyI; in contrast, for patients in the LNM-negative group, no significant difference was observed in terms of the prediction ability of the PTS scores in colon cancer with early T-stages on LI, VI, PI, or AnyI (**Table 4**).

DISCUSSION

In this study, we established a novel stromal microenvironment parameter—PTS score—to predict LNM in patients with colon cancer. To the best of our knowledge, this is the first study to develop a predictive histopathological parameter for LNM in patients with colon cancer by using artificial intelligence.

TABLE 2 | Predictive values of the PTS score for metastasis in colon cancer.

DSC score	mean (SD)	95% CIs	
		Lower	Upper
Adipose tissue	0.938 (0.141)	0.93	0.946
Lymphocytes	0.968 (0.055)	0.964	0.972
Mucus	0.841 (0.182)	0.83	0.852
Smooth muscle	0.732 (0.313)	0.707	0.758
Normal colon mucosa	0.928 (0.094)	0.921	0.935
Stroma	0.815 (0.235)	0.793	0.837
Colon cancer epithelium	0.930 (0.097)	0.925	0.936
Total	0.892 (0.179)	0.888	0.897

DSC, dice similarity coefficient; SD, standard deviation; CIs, confidence intervals.
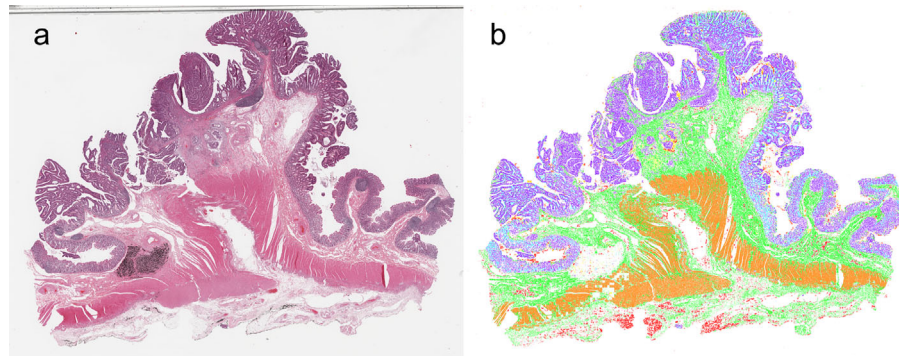
FIGURE 2 | Synthetic whole-slide images. **(A)** original pathology image. **(B)** Visualization of image segmentation by the model: colon cancer epithelium, purple; stroma, green; normal epithelium, light blue; muscle, orange; adipose tissue, red; lymphocyte, blue; mucus, yellow.
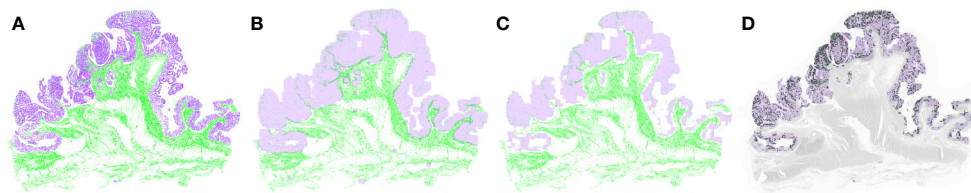
FIGURE 3 | Tumor and peri-tumoral stroma (PTS) segmentation after applying morphological image processing. **(A)** The model extracted the tumor and stromal portion from the whole-slide image. After the morphological dilation **(B)** and erosion operations **(C)**, the PTS area was segmented **(D)**. Purple represents tumor, and green represents PTS.

Considering the high interobserver variability in traditional pathological assessment (26–29), more accurate and reproducible histopathological assessments can reduce the inaccuracies associated with relying on subjective individual markers and better define the optimal treatment strategy for colon cancer. Whole-slide images (WSIs) contain a vast amount of information regarding cancer patients; however, it can be difficult to assess all features through manual evaluation of histology tissues, because it is significantly time consuming and can lead to substantial intra- and inter-observation variations among pathologists (30–32).

To date, a few parameters for assessing the prognosis of patients with colon cancer have been developed using computer-aided CNN methods from pathologic images (18, 33–35). In a recent German study, Kather et al. developed a parameter, the so-called "deep stroma score," to predict the prognosis of overall survival directly from histopathological images in CRC patients (18). However, it comprised information from not only stroma (cancer-related or not cancer-related stroma) but also various other components such as debris and adipose tissue, regardless of their distance from the tumor (18). The tumor microenvironment is a heterogeneous population of cells composed of tumor cells and tumor-associated stroma, which promote tumor growth, development, and propagation, surrounding non-cancer or stromal cells recruited by the tumor (36–39). Therefore, an analysis focused on the stromal components near a tumor could appropriately assess the contribution of cancer-related stroma in cancer tissue.

Another study by Takamatsu et al. presented a deep-learning model for predicting LNM from pathology images with cytokeratin immunohistochemistry in early CRC (33). However, only a limited number of LNM events exist, which limited the data available for the study, caused by the low rate of metastasis in early CRC. Furthermore, stepwise procedures, such as cytokeratin immunohistochemical staining and calculation of several parameters followed by model selection, were necessary for the prediction. Thus, it is inconvenient and not applicable for unusual cases that lack typical histological features in a slide image. A recent Chinese study also presented several morphologic parameters from pathology data to predict recurrent risk in stage III CRC (34). The authors generated new parameters by combining different histological components from whole tissue slides. Although this might be an interesting attempt, the validity of the parameters is not guaranteed considering the variability of tissue components contained in histological images through the pathology preparation. Lastly, Bychkov et al. stratified CRC patients for disease-specific survival into low- and high-risk groups using a CNN method on pathology images (35). However, they did not present any specific histological prognostic parameter, which could have potential utility in clinical decision-making.

Several previous studies have revealed prognostic information regarding the tumor-stroma ratio in CRC (40–46). Despite the evidence, it has not been implemented in routine pathology reporting because of significant variations in methodology and

TABLE 3 | Predictive values of the PTS score for metastasis in colon cancer.

PTS score		mean (SD)	P-value	Univariate logistic regression			
				OR	95% CIs		P-value
LNM			<0.001				<0.001
	Negative	0.228 (0.160)			Ref.		
	Positive	0.380 (0.285)		29.654	5.677	196.987	
LI			0.004				0.002
	no	0.245 (0.163)			Ref.		
	yes	0.380 (0.308)		14.199	2.992	82.384	
PI			0.469				0.463
	no	0.258 (0.185)			Ref.		
	yes	0.228 (0.186)		0.369	0.019	4.283	
VI			0.274				0.159
	no	0.272 (0.186)			Ref.		
	yes	0.334 (0.328)		2.927	0.635	13.459	
AnyI			0.040				0.035
	no	0.255 (0.168)			Ref.		
	yes	0.337 (0.287)		5.050	1.200	24.847	

PTS, peri-tumoral stroma; SD, standard deviation; OR, odds ratio; CIs, confidence intervals; LNM, lymph node metastasis; Ref., reference; LI, lymphatic invasion; PI, perineural invasion; VI, venous invasion; AnyI, any feature of extramural tumor deposits.

TABLE 4 | Predictive values of the PTS score for metastasis stratified by T stage in colon cancer.

PTS score		T0, T1, T2					T3, T4				
		Univariate logistic regression					Univariate logistic regression				
		mean (SD)	p-value	OR	95% CIs	P-value	mean (SD)	p-value	OR	95% CIs	P-value
LI			0.524			0.511		0.005			0.003
	no	0.244 (0.191)			Ref.		0.246 (0.153)			Ref.	
	yes	0.300 (0.182)		4.568	0.035 445.833		0.391 (0.320)		16.415	2.912 124.106	
PI			NA			NA		0.661			0.659
	no	0.267 (0.180)			Ref.		0.255 (0.189)			Ref.	
	yes	0.045 (NA)		NA	NA NA		0.235 (0.186)		0.549	0.029 6.678	
VI			0.143			0.271		0.248			0.156
	no	0.246 (0.175)			Ref.		0.281 (0.190)			Ref.	
	yes	0.133 (0.090)		0.001	0.000 12.905		0.351 (0.336)		3.106	0.642 15.753	
AnyI			0.903			0.895		0.041			0.049
	no	0.253 (0.186)			Ref.		0.256 (0.161)			Ref.	
	yes	0.263 (0.192)		1.356	0.009 111.014		0.345 (0.296)		5.529	1.123 34.79	

PTS, peri-tumoral stroma; SD, standard deviation; OR, odds ratio; CIs, confidence intervals; Ref., reference; LI, lymphatic invasion; PI, perineural invasion; VI, venous invasion; AnyI, any feature of extramural tumor deposits.

the lack of a standardized procedure for assessing tumor-stroma ratios. Published studies propose manual assessments of the deepest point of tumor invasion (40–42, 45, 46), systematic random point assessment (43), and the use of a semi-automatic method combining human input and a deep-learning algorithm using WSIs (44). However, time- and labor-intensive manual evaluations by pathologists with expertise must take precedence in these methods.

To overcome the issues discussed above, herein we applied a scoring procedure in which the relative amounts of tumor and the PTS score, as a straightforward measure, were calculated and adjusted based on the entire tumor area in a WSI using a CNN. Even without deep domain knowledge and the experience to assess pathologic images, this allows for obtaining easy and reproducible quantification of PTS and has the potential to pave the way for the implementation of the PTS score in clinical practice.

Our findings also indicated that the PTS score may be an independent parameter for predicting the presence of EMTDs in colon cancer. Histopathological identification of LI, VI, and PI in cancer tissue has long been recognized as a potential prognostic indicator for patient outcomes because of the likely association with progression to lymphatic metastasis (29, 47, 48). It is necessary to identify the parameters that can reduce interobserver variability because the rate of LI, VI, and PI detection is directly related to both technical aspects of tissue preparation, such as staining technique and the number of blocks examined, and the pathologist's experience and specialization (49, 50).

The present study demonstrated a significant association between the PTS score and LI and AnyI, whereas no

prognostic significance for VI and PI were found. Taken together, the PTS score could be a useful tool to identify patients who are at risk of developing LNM and EMTDs in colon cancer. Despite these advantages, the current study has a few limitations. One limitation of this study is that cases submitted for the TCGA database might be biased in terms of mainly including images in which the morphological patterns of disease are definitive, which could be different from what pathologists encounter in their daily practice. In addition, we could not alleviate the heterogeneity in stain color, despite the well-established stain normalization method. Therefore, it will be necessary to standardize a pathology stain method, which will decrease the difficulty of producing consistent diagnostic results and help build systems that generalize well. Another limitation is that, despite a good potential prognostic value of the PTS score for LNM and EMTDs overall and in T3–4 colon cancer patients, a prognostic value for cases with early T-stages was not observed. This may result from a class imbalance problem due to the limited sample size and the low event rate of EMTDs. Therefore, further studies should be performed using larger samples to obtain more accurate results for early T-stage colon cancer.

In conclusion, we established that the PTS score is, potentially, a promising and easy-to-apply prognostic parameter for LNM in colon cancer. However, because of the limitations inherent in studies based on observational data, these findings should be confirmed through subsequent prospective clinical trials.

DATA AVAILABILITY STATEMENT

The datasets presented in this study can be found in online repositories. The names of the repository/repositories and accession number(s) can be found in the article/**Supplementary Material**.

ETHICS STATEMENT

This study was reviewed and approved by the Institutional Review Board of the Kyung Hee University Hospital at Gangdong (KHNMC IRB 2020-09-025). The need for informed consent was waived because all data used in this study were de-identified.

AUTHOR CONTRIBUTIONS

FUNDING

ACKNOWLEDGMENTS

SUPPLEMENTARY MATERIAL

The Supplementary Material for this article can be found online at: https://www.frontiersin.org/articles/10.3389/fonc.2020.619803/full#supplementary-material

SUPPLEMENTARY FIGURE 1 | Overview of the analysis pipeline.

SUPPLEMENTARY FIGURE 2 | Performance plot of the proposed convolutional neural network model showing training accuracy (green line), test accuracy (yellow line), training loss (red line), and test loss (blue line).

SUPPLEMENTARY FIGURE 3 | Estimated binormal ROC curve (bold) and the 95% confidence bands (stepped red line) of the ROC curve for assessing the predictive value of the peri-tumoral stroma score.

SUPPLEMENTARY FIGURE 4 | Differences of the peri-tumoral stroma score according to the status of extramural tumor deposits in colon cancer (*$P \leq 0.05$; **$P \leq 0.01$).

REFERENCES

1. Bray F, Ferlay J, Soerjomataram I, Siegel RL, Torre LA, Jemal A. Global cancer statistics 2018: GLOBOCAN estimates of incidence and mortality worldwide for 36 cancers in 185 countries. *CA Cancer J Clin* (2018) 68:394–424. doi: 10.3322/caac.21492

2. Siegel RL, Miller KD, Jemal A. Cancer Statistics, 2017. *CA Cancer J Clin* (2017) 67:7–30. doi: 10.3322/caac.21387

3. Logan RF, Patnick J, Nickerson C, Coleman L, Rutter MD, von Wagner C. Outcomes of the Bowel Cancer Screening Programme (BCSP) in England after the first 1 million tests. *Gut* (2012) 61:1439–46. doi: 10.1136/gutjnl-2011-300843

4. Inadomi JM. Screening for Colorectal Neoplasia. *N Engl J Med* (2017) 376:149–56. doi: 10.1056/NEJMcp1512286

5. Gunderson LL, Jessup JM, Sargent DJ, Greene FL, Stewart AK. Revised TN categorization for colon cancer based on national survival outcomes data. *J Clin Oncol* (2010) 28:264–71. doi: 10.1200/jco.2009.24.0952

6. Sargent D, Shi Q, Yothers G, Van Cutsem E, Cassidy J, Saltz L, et al. Two or three year disease-free survival (DFS) as a primary end-point in stage III adjuvant colon cancer trials with fluoropyrimidines with or without oxaliplatin or irinotecan: data from 12,676 patients from MOSAIC, X-ACT, PETACC-3, C-06, C-07 and C89803. *Eur J Cancer (Oxford Engl 1990)* (2011) 47:990–6. doi: 10.1016/j.ejca.2010.12.015

7. Sargent D, Sobrero A, Grothey A, O'Connell MJ, Buyse M, Andre T, et al. Evidence for cure by adjuvant therapy in colon cancer: observations based on individual patient data from 20,898 patients on 18 randomized trials. *J Clin Oncol* (2009) 27:872–7. doi: 10.1200/jco.2008.19.5362

8. Pelkey TJ, Frierson HFJr., Bruns DE. Molecular and immunological detection of circulating tumor cells and micrometastases from solid tumors. *Clin Chem* (1996) 42:1369–81. doi: 10.1093/clinchem/42.9.1369

9. Weaver DL. Sentinel lymph nodes and breast carcinoma: which micrometastases are clinically significant? *Am J Surg Pathol* (2003) 27:842–5. doi: 10.1097/00000478-200306000-00018

10. Liefers GJ, Cleton-Jansen AM, van de Velde CJ, Hermans J, van Krieken JH, Cornelisse CJ, et al. Micrometastases and survival in stage II colorectal cancer. *N Engl J Med* (1998) 339:223–8. doi: 10.1056/nejm199807233390403

11. Koyanagi K, Bilchik AJ, Saha S, Turner RR, Wiese D, McCarter M, et al. Prognostic relevance of occult nodal micrometastases and circulating tumor cells in colorectal cancer in a prospective multicenter trial. *Clin Cancer Res* (2008) 14:7391–6. doi: 10.1158/1078-0432.Ccr-08-0290

12. Waldman SA, Hyslop T, Schulz S, Barkun A, Nielsen K, Haaf J, et al. Association of GUCY2C expression in lymph nodes with time to recurrence and disease-free survival in pN0 colorectal cancer. *Jama* (2009) 301:745–52. doi: 10.1001/jama.2009.141

13. Hipp J, Flotte T, Monaco J, Cheng J, Madabhushi A, Yagi Y, et al. Computer aided diagnostic tools aim to empower rather than replace pathologists: Lessons learned from computational chess. *J Pathol Inform* (2011) 2:25. doi: 10.4103/2153-3539.82050

14. Hamilton PW, Bankhead P, Wang Y, Hutchinson R, Kieran D, McArt DG, et al. Digital pathology and image analysis in tissue biomarker research. *Methods (San Diego Calif)* (2014) 70:59–73. doi: 10.1016/j.ymeth.2014.06.015

15. Link KH, Staib L, Kreuser ED, Beger HG. Adjuvant treatment of colon and rectal cancer: impact of chemotherapy, radiotherapy, and immunotherapy on routine postsurgical patient management. Forschungsgruppe Onkologie Gastrointestinaler Tumoren (FOGT). *Recent Results Cancer Res* (1996) 142:311–52. doi: 10.1007/978-3-642-80035-1_19

16. Edge SB, Byrd DR, Carducci MA, Compton CC, Fritz A, Greene F. *AJCC cancer staging manual*. New York City, USA: Springer New York (2010).

17. Wünsch K, Müller J, Jähnig H, Herrmann RA, Arnholdt HM, Märkl B. Shape is not associated with the origin of pericolonic tumor deposits. *Am J Clin Pathol* (2010) 133:388–94. doi: 10.1309/ajcpawolx7adzq2k

18. Kather JN, Krisam J, Charoentong P, Luedde T, Herpel E, Weis CA, et al. Predicting survival from colorectal cancer histology slides using deep learning: A retrospective multicenter study. *PloS Med* (2019) 16:e1002730. doi: 10.1371/journal.pmed.1002730

19. Ronneberger O, Fischer P, Brox T. U-net: Convolutional networks for biomedical image segmentation. In: *International Conference on Medical image computing and computer-assisted intervention*. USA: Springer (2015). p. 234–41. doi: 10.1007/978-3-319-24574-4_28

20. Macenko M, Niethammer M, Marron JS, Borland D, Woosley JT, Guan X, et al. A method for normalizing histology slides for quantitative analysis. In: *2009 IEEE International Symposium on Biomedical Imaging: From Nano to Macro*. USA: IEEE (2009). p. 1107–10. doi: 10.1109/ISBI.2009.5193250

21. Otsu, N.J.I.T.o.S., Man and Cybernetics. A Threshold Selection Method from Gray-Level Histograms. IEEE Transactions on Systems, Man, and Cybernetics: Systems (1979) 9:62–6. doi: 10.1109/TSMC.1979.4310076

22. Konur O, Kingma D, Ba J. Adam: A Method for Stochastic Optimization. In: *International Conference on Learning Representations*. International Conference on Learning Representations (2015).

23. Gonzalez RC, Woods RE, Eddins SL. *Digital image processing using MATLAB*. India: Pearson Education India (2004).

24. Raid A, Khedr W, El-Dosuky MAoud, M.J.I.J.o.C.S., Engineering and Technology, I. Image restoration based on morphological operations. *Int J Sci Res CSE & IT* (2014) 4:9–21. doi: 10.5121/ijcseit.2014.4302

25. Compton CC, Byrd DR, Garcia-Aguilar J, Kurtzman SH, Olawaiye A, Washington MK. *AJCC cancer staging atlas: a companion to the seventh editions of the AJCC cancer staging manual and handbook*. Berlin/Heidelberg, Germany: Springer Science & Business Media (2012). doi: 10.1007/978-1-4614-2080-4

26. Xu F, Xu J, Lou Z, Di M, Wang F, Hu H, et al. Micropapillary component in colorectal carcinoma is associated with lymph node metastasis in T1 and T2 Stages and decreased survival time in TNM stages I and II. *Am J Surg Pathol* (2009) 33:1287–92. doi: 10.1097/PAS.0b013e3181a5387b

27. Bosch SL, Teerenstra S, de Wilt JH, Cunningham C, Nagtegaal ID. Predicting lymph node metastasis in pT1 colorectal cancer: a systematic review of risk factors providing rationale for therapy decisions. *Endoscopy* (2013) 45:827–34. doi: 10.1055/s-0033-1344238

28. Glasgow SC, Bleier JI, Burgart LJ, Finne CO, Lowry AC. Meta-analysis of histopathological features of primary colorectal cancers that predict lymph node metastases. *J Gastroinest Surg* (2012) 16:1019–28. doi: 10.1007/s11605-012-1827-4

29. Harris EI, Lewin DN, Wang HL, Lauwers GY, Srivastava A, Shyr Y, et al. Lymphovascular invasion in colorectal cancer: an interobserver variability study. *Am J Surg Pathol* (2008) 32:1816–21. doi: 10.1097/PAS.0b013e3181816083

30. Dalton LW, Pinder SE, Elston CE, Ellis IO, Page DL, Dupont WD, et al. Histologic grading of breast cancer: linkage of patient outcome with level of pathologist agreement. *Mod Pathol* (2000) 13:730–5. doi: 10.1038/modpathol.3880126

31. Albert R, Müller JG, Kristen P, Harms H. Objective nuclear grading for node-negative breast cancer patients: comparison of quasi-3D and 2D image-analysis based on light microscopic images. *Lab Invest J Tech Methods Pathol* (1998) 78:247–59.

32. Roberts CA, Beitsch PD, Litz CE, Hilton DS, Ewing GE, Clifford E, et al. Interpretive disparity among pathologists in breast sentinel lymph node evaluation. *Am J Surg* (2003) 186:324–9. doi: 10.1016/s0002-9610(03)00268-x

33. Takamatsu M, Yamamoto N, Kawachi H, Chino A, Saito S, Ueno M, et al. Prediction of early colorectal cancer metastasis by machine learning using digital slide images. *Comput Methods Programs Biomed* (2019) 178:155–61. doi: 10.1016/j.cmpb.2019.06.022

34. Jiang D, Liao J, Duan H, Wu Q, Owen G, Shu C, et al. A machine learning-based prognostic predictor for stage III colon cancer. *Sci Rep* (2020) 10:10333. doi: 10.1038/s41598-020-67178-0

35. Bychkov D, Linder N, Turkki R, Nordling S, Kovanen PE, Verrill C, et al. Deep learning based tissue analysis predicts outcome in colorectal cancer. *Sci Rep* (2018) 8:3395. doi: 10.1038/s41598-018-21758-3

36. Kidd S, Spaeth E, Watson K, Burks J, Lu H, Klopp A, et al. Origins of the tumor microenvironment: quantitative assessment of adipose-derived and bone marrow-derived stroma. *PloS One* (2012) 7:e30563. doi: 10.1371/journal.pone.0030563

37. Hanahan D, Coussens LM. Accessories to the crime: functions of cells recruited to the tumor microenvironment. *Cancer Cell* (2012) 21:309–22. doi: 10.1016/j.ccr.2012.02.022

38. Gupta GP, Massagué J. Cancer metastasis: building a framework. *Cell* (2006) 127:679–95. doi: 10.1016/j.cell.2006.11.001

39. Valastyan S, Weinberg RA. Tumor metastasis: molecular insights and evolving paradigms. *Cell* (2011) 147:275–92. doi: 10.1016/j.cell.2011.09.024

40. Scheer R, Baidoshvili A, Zoidze S, Elferink MAG, Berkel AEM, Klaase JM, et al. Tumor-stroma ratio as prognostic factor for survival in rectal adenocarcinoma: A retrospective cohort study. *World J Gastroinest Oncol* (2017) 9:466–74. doi: 10.4251/wjgo.v9.i12.466

41. Huijbers A, Tollenaar RA, v Pelt GW, Zeestraten EC, Dutton S, McConkey CC, et al. The proportion of tumor-stroma as a strong prognosticator for stage II and III colon cancer patients: validation in the VICTOR trial. *Ann Oncol* (2013) 24:179–85. doi: 10.1093/annonc/mds246

42. Park JH, Richards CH, McMillan DC, Horgan PG, Roxburgh CSD. The relationship between tumour stroma percentage, the tumour microenvironment and survival in patients with primary operable colorectal cancer. *Ann Oncol* (2014) 25:644–51. doi: 10.1093/annonc/mdt593

43. West NP, Dattani M, McShane P, Hutchins G, Grabsch J, Mueller W, et al. The proportion of tumour cells is an independent predictor for survival in colorectal cancer patients. *Br J Cancer* (2010) 102:1519–23. doi: 10.1038/sj.bjc.6605674

44. Geessink OGF, Baidoshvili A, Klaase JM, Ehteshami Bejnordi B, Litjens GJS, van Pelt GW, et al. Computer aided quantification of intratumoral stroma yields an independent prognosticator in rectal cancer. *Cell Oncol (Dordrecht)* (2019) 42:331–41. doi: 10.1007/s13402-019-00429-z

45. Mesker WE, Junggeburt JM, Szuhai K, de Heer P, Morreau H, Tanke HJ, et al. The carcinoma-stromal ratio of colon carcinoma is an independent factor for survival compared to lymph node status and tumor stage. *Cell Oncol* (2007) 29:387–98. doi: 10.1155/2007/175276

46. van Pelt GW, Hansen TF, Bastiaannet E, Kjær-Frifeldt S, van Krieken J, Tollenaar R, et al. Stroma-high lymph node involvement predicts poor survival more accurately for patients with stage III colon cancer. *J Med Surg Pathol* (2016) 1:1000116. doi: 10.4172/2472-4971.1000116

47. Lim SB, Yu CS, Jang SJ, Kim TW, Kim JH, Kim JC. Prognostic significance of lymphovascular invasion in sporadic colorectal cancer. *Dis Colon Rectum* (2010) 53:377–84. doi: 10.1007/DCR.0b013e3181cf8ae5

48. Liebig C, Ayala G, Wilks J, Verstovsek G, Liu H, Agarwal N, et al. Perineural invasion is an independent predictor of outcome in colorectal cancer. *J Clin Oncol* (2009) 27:5131–7. doi: 10.1200/jco.2009.22.4949

49. Compton C, Fenoglio-Preiser CM, Pettigrew N, Fielding LPJC. American joint committee on cancer prognostic factors consensus conference: colorectal working group. *Cancer* (2000) 88:1739–57. doi: 10.1002/(SICI)1097-0142 (20000401)88:7<1739::AID-CNCR30>3.0.CO;2-T

50. Kirsch R, Messenger DE, Riddell RH, Pollett A, Cook M, Al-Haddad S, et al. Venous invasion in colorectal cancer: impact of an elastin stain on detection and interobserver agreement among gastrointestinal and nongastrointestinal pathologists. *Am J Surg Pathol* (2013) 37:200–10. doi: 10.1097/PAS.0b013e31826a92cd

Conflict of Interest: The authors declare that the research was conducted in the absence of any commercial or financial relationships that could be construed as a potential conflict of interest.